Jahn, S., Wunder, B. (2009): Lithium speciation in aqueous fluids at high P and T studied by ab initio molecular dynamics and consequences for Li-isotope fractionation between minerals and fluids. - Geochimica et Cosmochimica Acta, 73, 18, 5428-5434

DOI: 10.1016/j.gca.2009.06.017

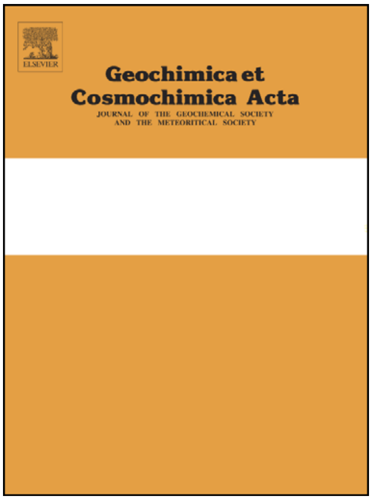

Lithium speciation in aqueous fluids at high *P* and *T* studied by *ab initio* molecular dynamics and consequences for Li-isotope fractionation between minerals and fluids

Sandro Jahn, Bernd Wunder

PII: S0016-7037(09)00415-3
DOI: 10.1016/j.gca.2009.06.017
Reference: GCA 6343

To appear in: *Geochimica et Cosmochimica Acta*

Received Date: 6 February 2009
Accepted Date: 12 June 2009

Please cite this article as: Jahn, S., Wunder, B., Lithium speciation in aqueous fluids at high *P* and *T* studied by *ab initio* molecular dynamics and consequences for Li-isotope fractionation between minerals and fluids, *Geochimica et Cosmochimica Acta* (2009), doi: 10.1016/j.gca.2009.06.017

Lithium speciation in aqueous fluids at high *P* and *T* studied by *ab initio* molecular dynamics and consequences for Li-isotope fractionation between minerals and fluids

Sandro Jahn* and Bernd Wunder

Deutsches GeoForschungsZentrum GFZ, Section 3.3, Telegrafenberg, 14473 Potsdam, Germany

*Corresponding author. E-mail address: jahn@gfz-potsdam.de

Abstract

Ab initio molecular dynamics simulations are performed to study the speciation changes in lithium bearing aqueous fluids at high temperature (T=1000 K) and high pressures, P, between about 0.3 and 6.0 GPa. The simulations show a linear increase in Li coordination with fluid density, from 3.2 to about five in the considered pressure range. Towards low densities, associated LiF complexes are becoming increasingly stable, which is quantified by evaluating the dynamic behavior of the respective species. In the high-density region, HF complexes are observed. The differences in speciation may be related to structural changes of the solvent under compression. At a fluid density of 1.2 g/cm^3, kinks in the pressure dependences of the oxygen-oxygen nearest neighbor distance and the oxygen-oxygen coordination are observed, which indicates a change in compaction mechanism. Assuming that the Li coordination difference between crystal and fluid is a major determinant for the isotopic fractionation between minerals and fluids, we expect only a small pressure dependence of the Li isotopic fractionation

between Li bearing fluids and minerals. Our simulation results are consistent with experimental data that show reverse fractionation of ^{7}Li between fluid and mineral, when Li is in tetrahedral instead of octahedral coordination in the crystal.

1. INTRODUCTION

Aqueous fluids are involved in most geochemical processes in the Earth's crust but they are also very important at larger depth, especially in the vicinity of subduction zones (Manning, 2004). In the presence of fluids, many physical properties of rocks are altered substantially. For instance, fluids are thought to be responsible for the mechanical softening or the partial melting of mantle rocks, which is related to the generation of mantle-derived magmas (Ulmer, 2001). In addition, fluids are excellent media for chemical transport (Brenan et al., 1998).

One key parameter for understanding, e.g., the solubility of minerals in fluids, diffusion rates for chemical transport, the electrical conductivity, or the partitioning of elements between fluids and rocks is the speciation of solutes in aqueous fluids. The characterization of these fluids under relevant geological conditions requires *in situ* experimental methods due to the strong dependence of the fluid properties on pressure, P, and temperature, T. Nevertheless, the measured data often provide only indirect information on speciation and are therefore difficult to interpret. Atomic scale simulations are a powerful complementary tool to get more direct insight into the microscopic structure and dynamics in fluids.

Lithium is an important element used as a geochemical tracer for mass transfer during geological processes, e.g. at convergent margins. For a quantitative understanding of these processes, the isotopic fractionation of its isotopes between minerals and fluids needs to be studied. Isotopic fractionation of lithium, which occurs in subduction zone regions by fluids expelled from the slab and mineral restite, diminishes with increasing temperature and is assumed to be independent on pressure. By breakdown of OH-bearing minerals during the subduction process, lithium isotope fractionations are produced due to preferential incorporation of ^{7}Li into expelled fluids relative to most silicates, except for staurolite (Wunder et al., 2007).

Isotopic fractionation of cations between two phases is driven by differences in the respective chemical potentials, which may be represented by energetic differences of their bonding environments. In general, for phases having different Li-coordination, the lighter isotope preferentially occupies the higher coordinated site (Schauble, 2004). In most silicates that occur at larger slab depths the coordination of lithium is octahedral, except in staurolite (Dutrow, 1991) and amphibole (Wenger and Armbruster, 1991). Aqueous fluids are usually thought to contain four-fold coordinated $Li(H_2O)_4^+$ -clusters (Yamaji et al., 2001; Ikeda et al., 2007). However, the assumption that $Li(H_2O)_4^+$ -clusters are the main lithium species in such fluids is based on theoretical calculations at ambient conditions (Yamaji et al., 2001; Ikeda et al., 2007). It is unclear to what extent different cluster types with e.g. five or six water molecules, which occur as small amounts in fluids at ambient conditions, are relevant at high pressures and high temperatures. This question is especially interesting since the structure of the solvent (H_2O) changes significantly from the liquid to the supercritical state (Weingärtner and Franck, 2005). Experimental studies of this problem are difficult since conventional spectroscopic methods, e.g. *in situ* Raman spectroscopy at high *P* and *T*, are not sensitive to the speciation of lithium in fluids.

Here, we study the speciation of lithium in aqueous fluid at high *P* and *T* by *first-*

principles modeling, and discuss a possible pressure dependence of the isotopic fractionation of lithium caused by variation of the structural Li environment with pressure. *Ab initio* molecular dynamics (AIMD) simulations are performed to characterize the hydration of Li ions in aqueous fluids at T=1000 K as a function of pressure. Coordination and speciation changes are discussed with regard to changes of the solvent structure in the supercritical state. Finally, consistency of the simulation results with existing experimental data on the Li-isotopic fractionation factors between lithium bearing minerals and fluids at high pressures is discussed.

2. COMPUTATIONAL METHODS

Ab initio molecular dynamics (AIMD) simulations are based on a quantum-mechanical description of the electronic structure, usually within the density functional theory (DFT) (Hohenberg and Kohn, 1964; Kohn and Sham, 1965). This high level of theory is needed to describe accurately the particle interactions in complex chemical systems. Classical molecular dynamics (MD) using force fields that subsume the electronic effects in a simplified way into analytical functions are often used to study aqueous solutions close to ambient conditions (Egorov et al., 2003), but their predictive power towards complex formation and towards high pressures is expected to be rather limited. The MD approach is needed to sample the speciation in the high pressure fluid, which is difficult to achieve using *ab initio* based static energy calculations on molecular clusters (as used e.g. in Yamaji et al. (2001)).

Due to the computational expense of AIMD simulations, a relatively small system size of 64 water molecules and a single Li ion is chosen here. Charge compensation is achieved by adding one F or one OH anion to the system. Although this model system corresponds approximately to a 0.9 *m* aqueous solution, it will resemble a more dilute fluid since the formation of complex species involving more than a single Li cation is not possible by definition of the simulation cell. Most of the following results refer to the system containing the fluorine ion. The initial structure was taken from a classical MD simulation of pure H_2O using the SPC/E potential, to which the ions were added. The AIMD simulations are performed in the NVT ensemble using Car-Parrinello molecular dynamics (Car and Parrinello, 1985) as implemented in the CPMD code (Marx and Hutter, 2000). The constant temperature of T=1000 K is controlled by a Nosé-Hoover chain thermostat (Nosé and Klein, 1983; Hoover, 1985). A reasonable compromise between energy conservation und computational efficiency is obtained by using a fictitious electron mass of 600 a.u. and an integration time step of 0.12 fs. The plane-wave expansion of the Kohn-Sham orbitals is truncated at a cutoff energy of 70 Ry. The BLYP exchange correlation functional (Becke, 1988; Lee et al., 1988) is used in conjunction with Goedecker-type pseudopotentials (Goedecker et al., 1996). At each volume, short simulations of 3-4 ps are used for equilibration before production runs of at least 10 ps are started. Most of the following results are presented as a function of density, which is easliy calculated from a constant volume simulation. To make contact with experiment, pressure is estimated using the equation of state of pure H_2O (Wagner and Pruss, 2002). Since the uncertainty of this estimation is rather high at extreme conditions of pressure and temperature, the pressures shown in this paper have to be taken with care.

3. RESULTS

3.1 Solvent structure

The structure of the solvent is an important parameter that determines both coordination and speciation of the solute. Here, the solvent is supercritical water in the density range from 0.57 g/cm^3 to 1.42 g/cm^3, which at T=1000 K corresponds to pressures of about 0.3 GPa and 6.0 GPa, respectively. Its structural evolution with pressure is represented by the partial radial distribution functions, $g_{OH}(r)$ (Fig. 1) and $g_{OO}(r)$ (Fig. 2). As expected, increasing pressure leads to a shift of the intermolecular distances to smaller values. The shoulder at about 2 Å in $g_{OH}(r)$ indicates the presence of some kind of hydrogen bond but there is strong overlap with the dominating peak of non-hydrogen bonded O-H pairs at around 3 Å. Dynamic analysis of the respective O-H bonds reveals that structures responsible for the shoulder and the main peak have a maximum lifetime of not more than about 0.1 ps over the whole pressure range. Hence, if hydrogen bonding exists, it is very dynamic and bonds are continuously broken and reformed, which is consistent with previous computational studies (Boero et al., 2000).

The structural re-arrangement of the solvent molecules due to the densification of the fluid is further demonstrated by the change of the nearest neighbor oxygen-oxygen distance and the average oxygen coordination by oxygens as a function of fluid density (Fig. 3). The average O-O distances at each density are obtained from the positions of the first maxima of the respective partial radial distribution functions, $g_{OO}(r)$, shown in Fig. 2. Up to a fluid density of about 1.2 g/cm^3, the nearest neighbor O-O distance decreases linearly with density. Then, the slope of the curve changes and continues again with a linear dependence towards higher densities. The respective oxygen coordination increases to about 12.5 and reaches a plateau at densities above 1.2 g/cm^3.

3.2 Lithium coordination as a function of pressure

The hydration state of the Li$^+$ cation is described by the time average of the number of nearest neighbor water molecules. The average Li-O nearest neighbor distance is only weakly pressure dependent as illustrated by the radial distribution functions, $g_{LiO}(r)$, in Fig. 4. The first maximum of $g_{LiO}(r)$ is observed between 1.93 and 2.00 Å in the pressure range studied here with a weak decrease of distance towards higher pressures. This is consistent with Li-O distances in lithium inorganic salts, which range from 1.86 to 2.05 Å (Olsher et al., 1991). In these crystals, Li is either in tetrahedral or octahedral environment.

The position of the first minimum in $g_{LiO}(r)$ (see Fig. 4) is almost constant over the whole pressure range. Thus, a constant cutoff of 2.8 Å is used to count the number of nearest neighbor oxygen anions. The corresponding cutoff for the first neighbor Li-F distance is 2.3 Å. In Figure 5, we present results for the lithium coordination by anions, i.e. without distinction between different nearest neighbor anions (oxygen or fluorine) or nearest neighbor species (OH^- or H_2O) as functions of mass density and pressure. Average coordination numbers are also given in Fig. 5 and in Table 1.

Previous AIMD simulations show that at ambient conditions, Li is almost always coordinated by four water molecules (Ikeda et al., 2007). At the same density (=1.0 g/cm^3), we also observe a mean coordination number of about four (see Fig. 5 and Table 1), however with considerable proportions of three- and five-fold coordination (about 20% each). Only about 60% of the simulation period, the Li ion was in actual four-fold coordination. At T=1000 K, =1.0 g/cm^3 corresponds to a pressure of about 1.5 GPa. At lower pressures, the Li coordination drops considerably, which leads to a dominant three-fold coordination and a mean coordination of 3.2 at the lowest density. The Li coordination increases continuously with pressure and linearly with fluid density (Fig. 5). At the highest density (1.42 g/cm^3), the distribution has a peak at five-fold coordination and the three-fold coordination has almost disappeared. The Li coordination is apparently independent on the charge compensating anion, i.e. the results for the aqueous fluids containing LiF and LiOH are the same within the uncertainties of the calculations (see Fig. 5).

3.3 Speciation changes

The structural changes of the solvent are accompanied by speciation changes of the solutes (see Fig. 6 and Table 1). In the low-density region up to about 0.8 g/cm^3, Li and F tend to form associated neutral complexes of LiF. They are found to be present in the respective simulations for more than 50% of the total simulation time. In the two highest density simulations, i.e. at 1.3 and 1.4 g/cm^3, we find instead considerable portions of HF complexes (about 15% of the simulation time) but only negligible amounts of LiF (<1%). The formation of HF requires the dissociation of a water molecule into H^+ and OH^-. Part of the OH^- forms short-lived charge neutral LiOH species (see Table 1), but most of it remains free OH^-, which is not very stable either due to frequent hopping of protons. Fluctuations in the speciation, especially in the occurrence of associated species (see Table 1), are likely due to the finite size of the simulation cell and the finite simulation time. Longer simulation runs and/or larger cells would be needed for a more quantitative analysis of the relative occurrence of those species.

3.4 Li self-diffusion coefficients

Transport coefficients are important properties to understand the mobility of ions in the fluid. The self-diffusion coefficient of the Li ion, D_{Li}, is obtained from the slope of the mean square displacement using the Einstein relation (Allen and Tildesley, 1987)

$$2tD_{Li} = \frac{1}{3}\left\langle \left|\mathbf{r}(t) - \mathbf{r}(0)\right|^2 \right\rangle \tag{1}$$

where $\boldsymbol{r}(t)$ refers to the position of the Li ion at time t and the angular brackets denote a time average. Since there is only a single Li ion and due to the relatively short simulation run, the uncertainty on D_{Li} is rather large (see Fig. 7). Therefore, we are unable to present a reliable pressure dependence of the self-diffusion coefficient. However, we can compare the mean diffusion coefficient obtained at T=1000 K with low temperature data from NMR experiments and classical MD simulations on 1.7 m LiCl aqueous solutions (Egorov et al., 2003). Our predicted value is about one order of magnitude smaller than the extrapolation of the experimental curve assuming Arrhenius-like temperature dependence of the self-diffusion coefficient.

4. DISCUSSION AND CONCLUSIONS

We start our discussion with the structure of the solvent. It is known that the structure of supercritical water differs significantly from water at ambient conditions (Weingärtner and Franck, 2005). At ambient conditions, the water structure is characterized by an infinite tetrahedral network of hydrogen bonded water molecules. In the supercritical state the network structure is unstable, which results in very dynamic hydrogen bonds that are continuously broken and reformed (Boero et al., 2000). Our simulations are performed at higher temperature and in a wider pressure range but they essentially confirm the previous studies by Boero et al. (2000). At T=1000 K, the lifetime of hydrogen bonds is smaller than 0.1 ps, which corresponds to not more than a few O-H vibrations.

The fact that the distribution of instantaneous cation coordinations varies smoothly with fluid density in simulations of only about 10 ps and using a single cation (Fig. 5) suggests that the hydration shell must also be subject to a fast dynamic change. This is in contrast with the behavior at ambient conditions where the Li hydration is expected to be rather rigid (Ikeda et al., 2007).

The dynamic behavior of the first hydration shell of the Li ion is quantified by evaluation of the mean residence times of the different coordinating species. We construct a correlation function similar to that used in Jahn (2008). Here, this function describes the probability that a Li-O or Li-F bond still exists at time *t* after bond formation. As maximum bond lengths, the positions of the first mimima of the respective radial distribution functions, $g_{LiO}(r)$ at 2.8 Å (see Fig. 4) and $g_{LiF}(r)$ at 2.4 Å, are chosen. The decay function (see inset of Fig. 8) is then fitted by a stretched exponential function of the form $A\exp[-(t/\tau)^{\beta}]$, where *A* corresponds to the time averaged occurrence of this bond as given by the mean Li coordination numbers by O or F (see Table 1), and   and   are the relaxation time and the stretching parameter, respectively. For the Li-O bond,   was used as a free fit parameter, which varied between 1.3 and 1.7 with no significant influence on . Due to the low fraction of Li-F bonds,   was fixed to a constant value of 2.0 for the fit of the corresponding LiF decay function.

The relaxation time for the Li-O bond, which essentially describes the residence time of an H_2O in the first hydration shell, is almost independent on the fluid density and has a rather low value of about 1 ps at the high temperature considered here (Fig. 8). On the contrary, the stability of the Li-F bond increases significantly towards lower densities (Fig. 8), which is consistent with the tendency for association in low pressure and high temperature fluids (Manning, 2004).

Looking at the behavior over the whole density range considered here there seems to be a correlation between changes in the Li speciation and structural changes of the solvent. The change in slope of the O-O nearest neighbor distance and in the oxygen coordination (Fig. 3) occurs at a density of about 1.2 g/cm^3. While at lower densities the compression of the fluid is accompanied by oxygen coordination changes, which indicates structural rearrangements, the oxygen coordination is essentially constant towards higher fluid density. Together with the steeper slope of the O-O distance this indicates a change in compaction mechanism from structural rearrangements to bond shortening. Structural changes around a density of 1.2 g/cm^3 have also been reported for liquid water at high temperature (up to 573 K) (Kawamoto et al., 2004). Regarding Li speciation, we observe appreciable Li in 6-fold coordination only at densities above 1.2 g/cm^3. Furthermore, there may be a tendency to form HF species towards high pressures (see Table 1). However, more simulation work is needed to quantify these observations.

Finally, we discuss the relation between cation coordination and isotopic fractionation. Isotopic fractionation experiments between spodumene – fluid (Wunder et al., 2006) and mica – fluid (Wunder et al., 2007) showed *T*-dependent fractionation with preferential incorporation of ^{7}Li into the fluid. In both spodumene and mica, Li is found in six-fold coordination. Spodumene has a displacive phase transition from C2/c to P2$_1$/c at high pressures of 3.2 GPa at room-temperature (Arlt and Angel, 2000). However, the difference in the octahedral Li-configuration between these two polymorphs seems to be too small to have a considerable effect on the Li-isotopic fractionation. Thus, it was concluded from the experimental studies that Li should remain essentially in four-fold (or at least lower than six-fold) coordination in the fluid over the relevant pressure range up to 2.0 GPa. Differences in the bonding strengths of the Li-octahedra in mica and spodumene were assumed to account for the differences in the extent of Li-isotope fractionation for the two solid – fluid systems.

On the contrary, in Li-isotope fractionation experiments between staurolite – fluid (Wunder et al., 2007), all performed at higher pressures of 3.5 GPa, the heavy ^{7}Li preferentially fractionated into staurolite. Under the assumption that the coordination-dependence dominates the Li-isotope fractionation, i.e. neglecting other energetic differences in the Li-polyhedra/cluster of staurolite and fluid, one might expect that the Li-coordination in the fluid at the high pressures of the experiments was higher than that in staurolite, which has Li in tetrahedral four-fold coordination. If this reasoning is correct, the extent of isotopic fractionation of lithium between minerals and fluids should also depend on pressure.

Our simulation results are fully consistent with this simple picture. Up to a pressure of 2 GPa, which at 1000 K corresponds to a density of approximately 1.1 g/cm^3, the average Li coordination remains below 4.5 (see Table 1). This is much smaller than six in the corresponding minerals spodumene or mica. At the highest pressure considered here (6 GPa), the Li coordination in the fluid has increased to about five, which is still smaller than in the crystals. From the cation coordination change, at most a small pressure dependence of the Li isotope fractionation between Li bearing fluids and either spodumene or mica can be expected in the pressure range up to about 6 GPa. Preliminary experiments of our group indicate such small pressure dependence in the system spodumene–fluid, but further experiments are needed to draw a conclusive picture. On the other hand, the Li coordination in the fluid at 3.5 GPa is indeed larger than 4.0, which can explain the preferential fractionation of ^{7}Li into staurolite. An experiment at lower pressure with a fluid density of less than 1.0 g/cm^3 could reverse the sign of the fractionation coefficient.

In conclusion, a good characterization of fluid properties at high pressure and high temperature is indispensable to *understand* their important role in geological processes. In the case of Li bearing aqueous fluids considered here, the *ab initio* simulations have provided unique insight into the atomic scale structure and dynamics of the fluid at extreme conditions not easily accessible experimentally. The occurrence of different species and their dynamic stability as a function of pressure and (potentially) temperature is apparently closely related to the structure of the solvent, which is significantly different between the liquid state at ambient conditions and the supercritical state at high *P* and *T*. On the contrary, the mean Li coordination by anions seems to depend mainly on the density of the fluid. From the pressure dependence of the cation coordination in the fluid it seems possible to predict at least relative magnitudes and the sign of isotopic fractionation between fluids and minerals.

ACKNOWLEDGMENTS

We would like to thank the associate editor B. Mysen, A. Shakar, T. Ota and an anonymous reviewer for useful comments and suggestions during the reviewing process. We are grateful to the *John von Neumann Institute for Computing* (NIC) Jülich for providing computing time on the IBM Blue Gene/L JUBL and on the IBM p690 cluster JUMP. S.J. was supported by project JA 1469/4-1 of the German Science Foundation (DFG).

References

Allen M. P. and Tildesley D. J. (1987) *Computer simulations of liquids.* Oxford

University Press.

Arlt T. and Angel R. J. (2000) Displacive phase transitions in C-centred clinopyroxenes: spodumene, $LiScSi_2O_6$ and $ZnSiO_3$. *Phys. Chem. Minerals* **27**, 719–731.

Becke A. D. (1988) Density-functional exchange-energy approximation with correct asymptotic behavior. *Phys. Rev. A* **38**, 3098 – 3100.

Boero, M., Terakura, K., Ikeshoji, T., Liew, C. C., Parrinello, M., 2000. Hydrogen bonding and dipole moment of water at supercritical conditions: A first-principles molecular dynamics study. Phys. Rev. Lett. 85, 3245–3248.

Brenan J. M., Ryerson F. J. and Shaw H. F. (1998) The role of aqueous fluids in the slab-to-mantle transfer of boron, beryllium, and lithium during subduction: Experiments and models. *Geochim. Cosmochim. Acta* **62**, 3337–3347.

Car R. and Parrinello M. (1985) Unified approach for molecular dynamics and density functional theory. *Phys. Rev. Lett.* **55**, 2471–2474.

Dutrow B. (1991) The effects of A1 and vacancies on Li substitution in iron staurolite - a synthesis approach. *Am. Mineral.* **76**, 42–48.

Egorov A. V., Komolkin A. V., Chizhik V. I., Yushmanov P. V., Lyubartsev A. P. and Laaksonen, A. (2003) Temperature and concentration effects on Li^+-ion hydration. A molecular dynamics simulation study. *J. Phys. Chem. B* **107**, 3234–3242.

Goedecker S., Teter M. and Hutter J. (1996) Separable dual-space Gaussian pseudopotentials. *Phys. Rev. B* **54**, 1703–1710.

Hohenberg P. and Kohn W. (1964) Inhomogeneous electron gas. *Phys. Rev.* **136**, B864–B871.

Hoover W. G. (1985) Canonical dynamics: Equilibrium phase-space distributions. *Phys. Rev. A* **31**, 1695 – 1697.

Ikeda T., Boero M. and Terakura K. (2007) Hydration of alkali ions from first principles molecular dynamics revisited. *J. Chem. Phys.* **126**, 034501.

Jahn S. (2008) Atomic structure and transport properties of MgO-Al_2O_3 melts: A molecular dynamics simulation study. *Am. Mineral.* **93**, 1486–1492.

Kawamoto, T., Ochiai, S., Kagi, H., 2004. Changes in the structure of water deduced from the pressure dependence of the Raman OH frequency. J. Chem. Phys. 120, 5867–5870.

Kohn W. and Sham L. J. (1965) Self-consistent equations including exchange and correlation effects. *Phys. Rev.* **140**, A1133–A1138.

Lee C., Yang W. and Parr R. C. (1988) Development of the Colle-Salvetti correlation-energy formula into a functional of the electron density. *Phys. Rev. B* **37**, 785–789.

Manning C. E. (2004) The chemistry of subduction-zone fluids. *Earth Planet. Sci. Lett.* **223**, 1–16.

Marx D. and Hutter J. (2000) Ab initio molecular dynamics: Theory and implementation. In: Grotendorst, J. (Ed.), *Modern Methods and Algorithms of Quantum Chemistry*, Forschungszentrum Jülich, NIC Series. Vol. 1. pp. 301–449.

Nosé S. and Klein M. L. (1983) Constant pressure molecular dynamics for molecular systems. *Mol. Phys.* **50**, 1055–1076.

Olsher U., Izatt R. M., Bradshaw J. S. and Dalley N. K. (1991) Coordination chemistry of lithium ion: A crystal and molecular structure review. *Chem. Rev.* **91**, 137–164.

Schauble E. A. (2004) Applying stable isotope fractionation theory to new systems. *Rev. Mineral. Geochem.* **55**, 65–111.

Ulmer P. (2001) Partial melting in the mantle wedge - the role of H_2O in the genesis of mantle-derived â˜arc-relatedâ™ magmas. *Phys. Earth Planet. Int.* **127**, 215–232.

Wagner W. and Pruss A. (2002) The IAPWS formulation 1995 for the thermodynamic properties of ordinary water substance for general and scientific use. *J. Phys. Chem. Ref. Data* **31**, 387–535.

Weingärtner, H., Franck, E. U., 2005. Supercritical water as a solvent. Angew. Chem. Int. Ed. 44, 2672–2692.

Wenger M. and Armbruster T. (1991) Crystal-chemistry of lithium - oxygen coordination and bonding. *Eur. J. Mineral.* **3**, 387–399.

Wunder B., Meixner A., Romer R. L., Feenstra A., Schettler G. and Heinrich W. (2007) Lithium isotope fractionation between Li-bearing staurolite, Li-mica and aqueous fluids: An experimental study. *Chem. Geol.* **238**, 277–290.

Wunder B., Meixner A., Romer R. L. and Heinrich W. (2006) Temperature-dependent isotopic fractionation of lithium between clinopyroxene and high-pressure hydrous fluids. *Contrib. Mineral. Petrol.* **151**, 112–120.

Yamaji K., Makita Y., Watanabe H., Sonoda A., Kanoh H., Hirotsu T. and Ooi K. (2001) Theoretical estimation of lithium isotopic reduced partition function ratio for lithium ions in aqueous solution. *J. Phys. Chem. A* **105**, 602–613.

Table 1: Occurrence of different species as a function of density averaged over the duration of the simulations. The different Li and F species sum up to 1.0. Also given are the average Li coordinations by oxygen and by anions (O or F).

density (g/cm^3)	LiF	LiOH	HF	Li$^+$	F$^-$	Li by O	Li by O+F
1.416	0.01	0.02	0.15	0.97	0.84	4.88	4.89
1.319	0.00	0.02	0.14	0.98	0.86	4.78	4.78
1.231	0.06	0.00	0.03	0.94	0.91	4.50	4.56
1.078	0.31	0.01	0.04	0.68	0.65	3.91	4.22
1.010	0.00	0.00	0.04	1.00	0.96	4.12	4.12
0.948	0.00	0.09	0.33	0.91	0.67	3.98	3.98
0.839	0.64	0.00	0.02	0.36	0.34	3.15	3.80
0.746	0.63	0.01	0.02	0.36	0.35	2.93	3.56
0.566	0.79	0.00	0.02	0.21	0.19	2.45	3.24

Figure 1: Partial radial distribution function between O and H ions, $g_{OH}(r)$, as a function of pressure. The first peak at about 1.0 Å corresponds to the intramolecular O-H distance of the H_2O molecule.

Figure 2: Partial radial distribution function between O and O ions, $g_{OO}(r)$, as a function of pressure.

Figure 3: (top) Oxygen-oxygen nearest neighbor distance obtained from the position of the first maximum of the respective partial radial distribution function $g_{OO}(r)$ (symbols). The lines represent linear fits to the data in two different density regions. (bottom) Average number of oxygens in the first oxygen coordination shell, which extends up to the first minimum of the respective $g_{OO}(r)$.

Figure 4: Partial radial distribution function between Li and O ions, $g_{LiO}(r)$, as a function of pressure. The first minimum of $g_{LiO}(r)$ at about 2.8 Å is used as cutoff radius of the first coordination sphere.

Figure 5: (top) Distribution of Li coordination by nearest neighbor anions (oxygens or fluorines) as a function of mass density and estimated pressure. The Li ion and its first coordination shell is described as a complex $[Li(H_2O,OH,F)_n]$, which has a charge between 0.0 and +1.0. n is the number of nearest neighbor anions. The open and filled symbols refer to the LiF and LiOH simulations, respectively. (bottom) Average Li

coordination represented by open circles. The line is the corresponding linear regression curve.

Figure 6: Snapshots from the AIMD simulations illustrating the increase of Li coordination with pressure. At low pressures, a considerable amount of associated LiF species is observed (see left picture). The Li ions are shown as large green and the F as smaller blue balls. H_2O molecules in the first hydration shell of the Li ion are shown as balls and sticks (red – O, white – H) whereas other H_2O are represented by sticks only.

Figure 7: Self-diffusion coefficients of Li ions as a function of temperature. The AIMD simulation results at high temperature are compared to low *T* data from NMR experiments and classical MD simulations of 1.7 *m* LiCl aqueous solution by Egorov et al. (2003).

Figure 8: Relaxation times representing the mean residence time of an H_2O molecule in the first hydration shell of the Li cation and the mean lifetime of the LiF complex, respectively, as a function of fluid density. Lines are just a guide to the eyes. Inset: The solid line represents the decay function described in the text for Li-O bond and $=0.948$ g/cm^3, the dashed line is the fitted curve of a stretched exponential function.

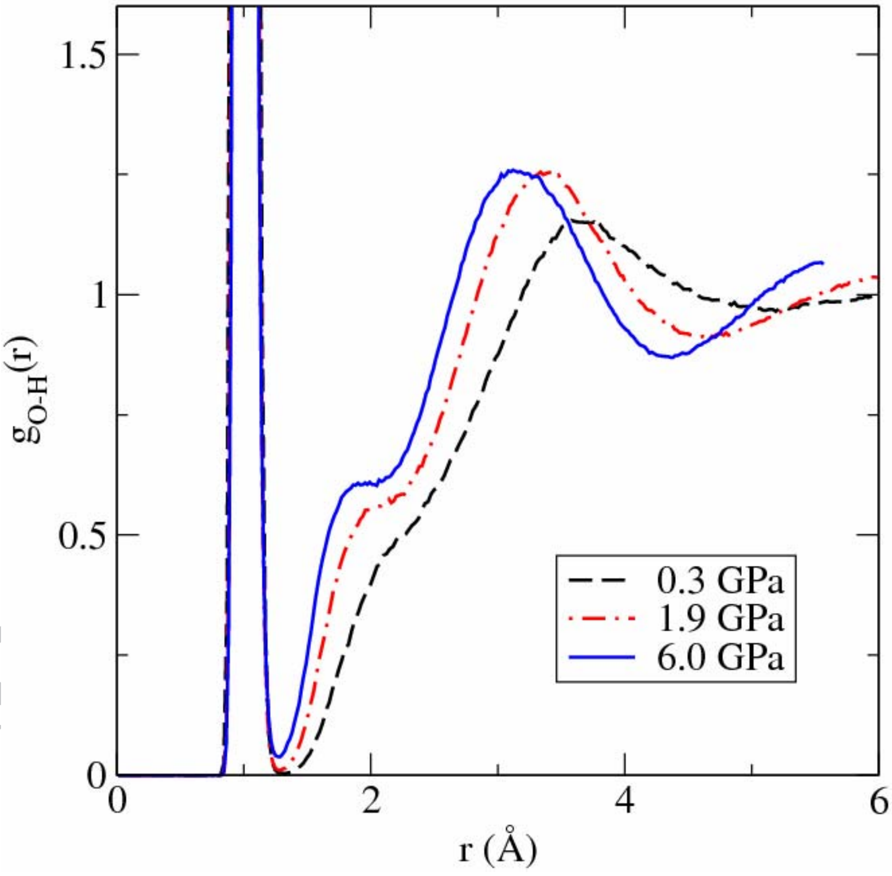

1.5
1
0.5
0
$g_{O\text{-}H}(r)$
0
2
4
6
r (Å)
0.3 GPa
1.9 GPa
6.0 GPa

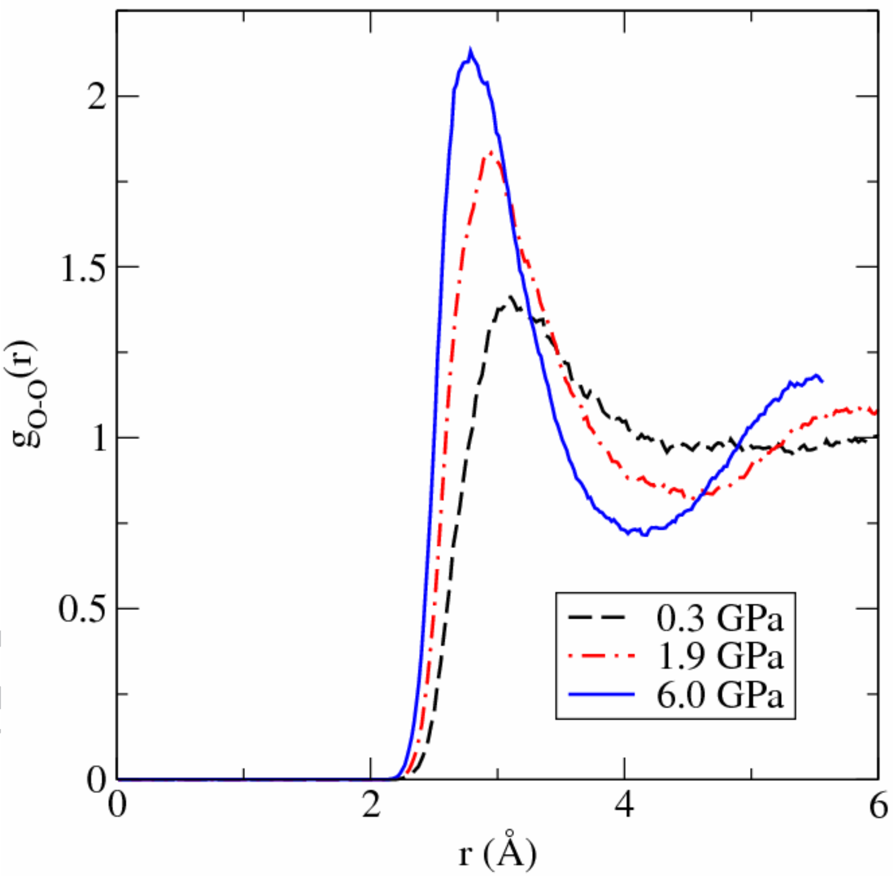

2
1.5
1
0.5
0
0
2
4
6
$g_{O-O}(r)$
r (Å)
0.3 GPa
1.9 GPa
6.0 GPa

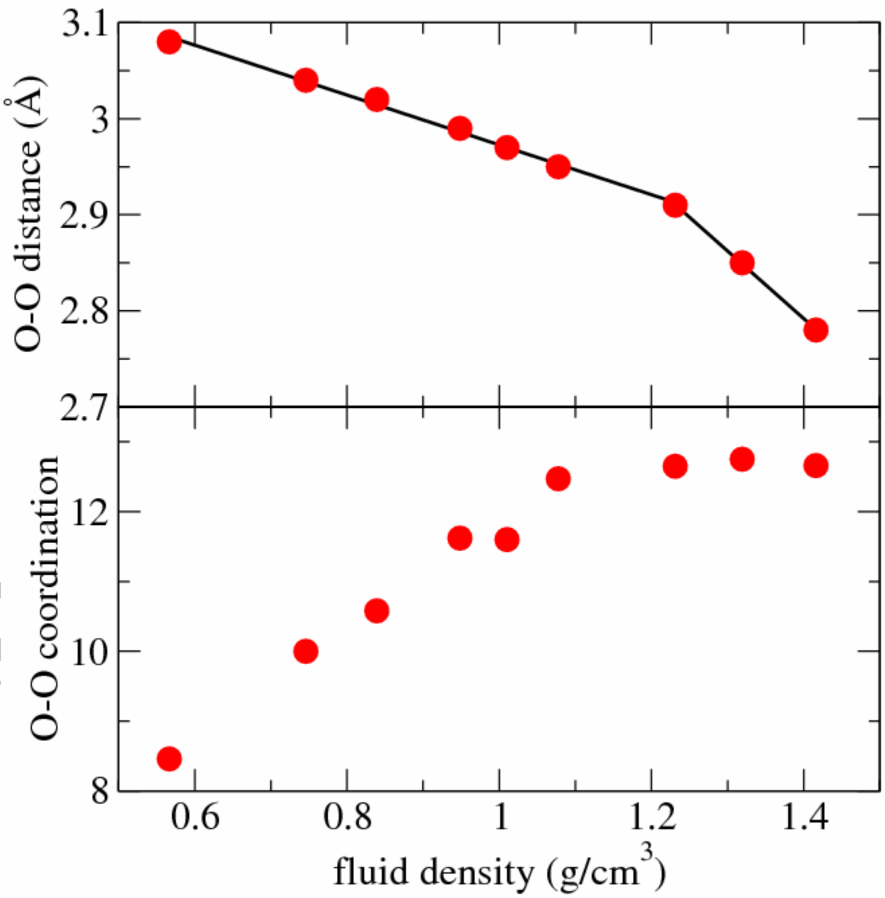
3.1
3
2.9
2.8
2.7
O-O distance (Å)
12
10
8
O-O coordination
0.6
0.8
1
1.2
1.4
fluid density (g/cm^3)

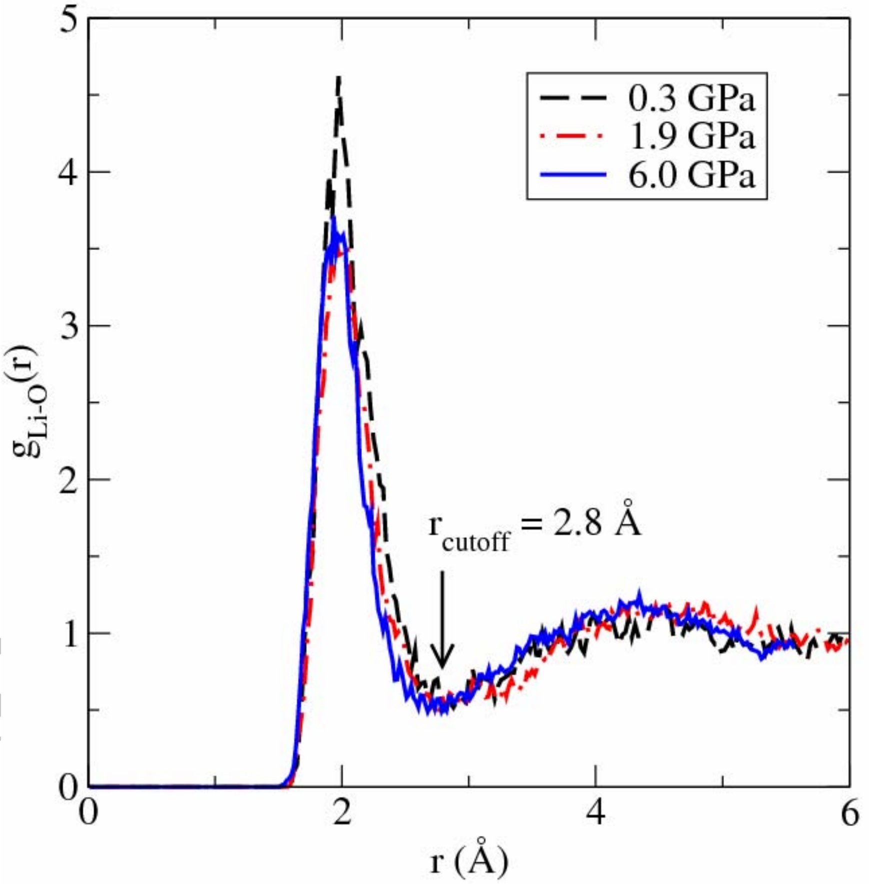
0.3 GPa
1.9 GPa
6.0 GPa
r_{cutoff} = 2.8 Å
$g_{Li\text{-}O}(r)$
r (Å)
0
1
2
3
4
5
0
2
4
6

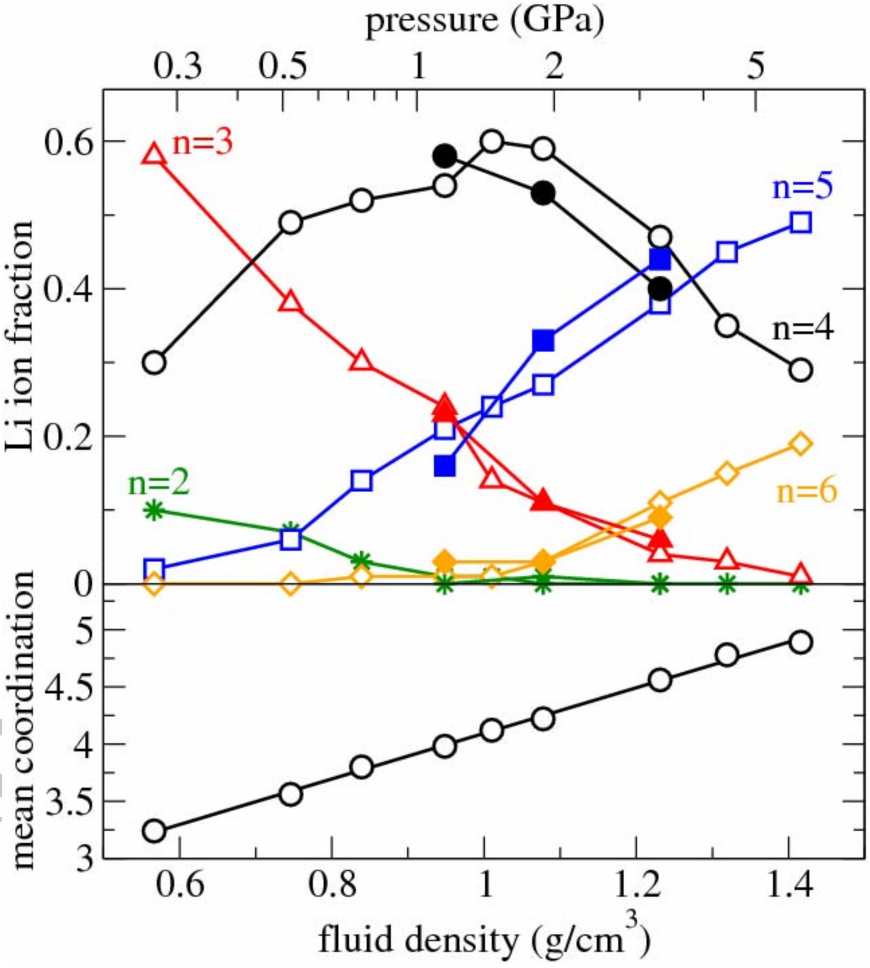
pressure (GPa)
0.3
0.5
1
2
5
Li ion fraction
0.6
0.4
0.2
0
n=3
n=5
n=4
n=2
n=6
mean coordination
5
4.5
4
3.5
3
0.6
0.8
1
1.2
1.4
fluid density (g/cm^3)

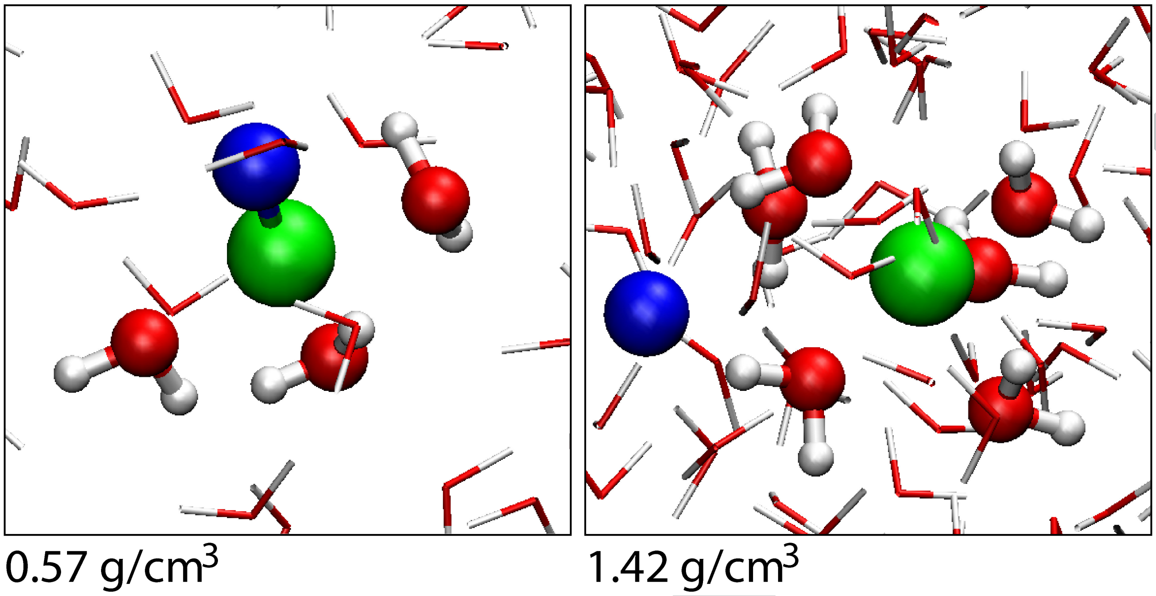
0.57 g/cm^3
1.42 g/cm^3

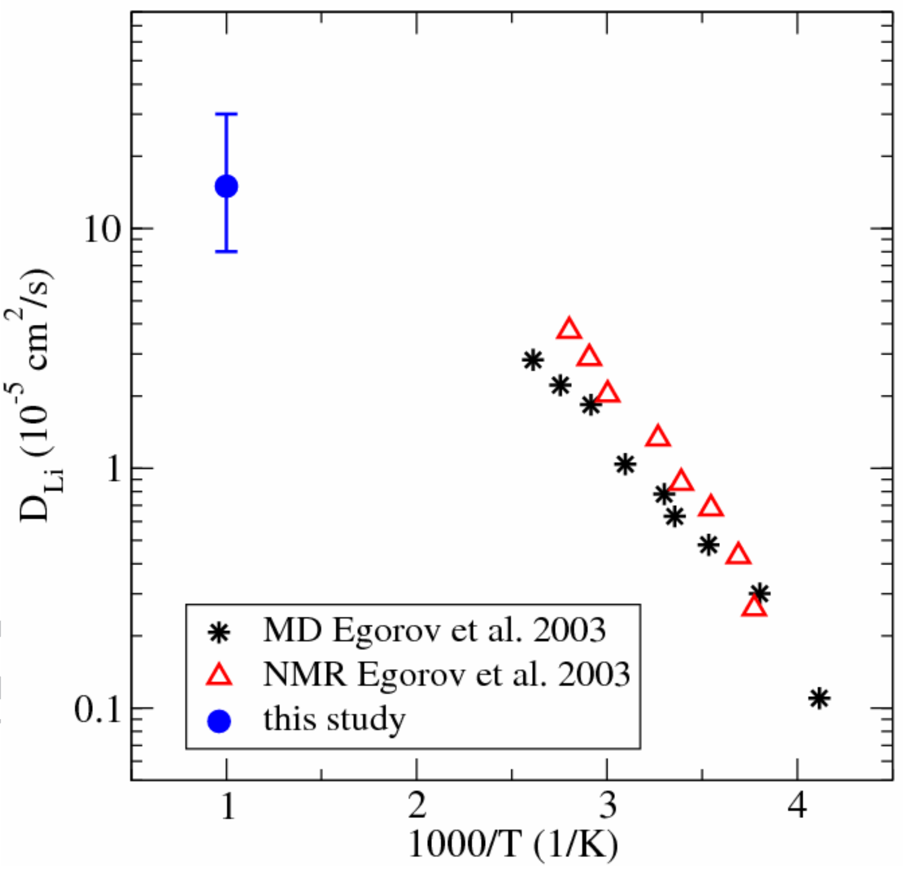

10
1
0.1
D_{Li} (10^{-5} cm^2/s)
1
2
3
4
1000/T (1/K)
MD Egorov et al. 2003
NMR Egorov et al. 2003
this study

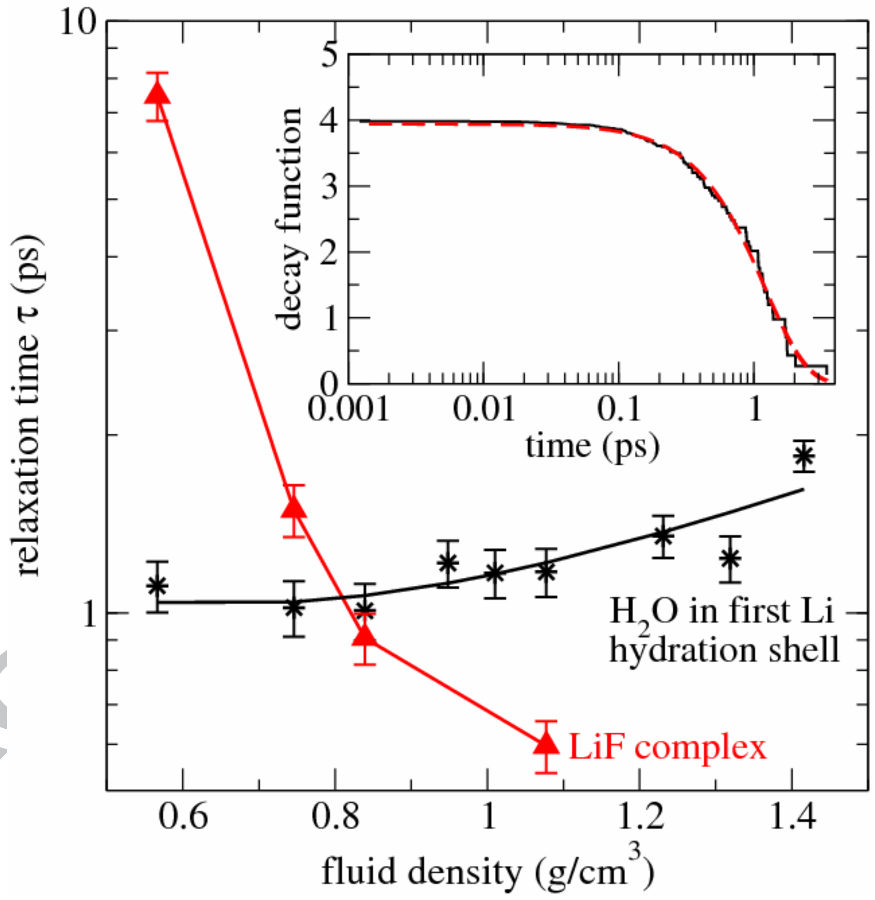
10
1
0.6
0.8
1
1.2
1.4
relaxation time τ (ps)
fluid density (g/cm^3)
H_2O in first Li hydration shell
LiF complex
5
4
3
2
1
0
0.001
0.01
0.1
1
decay function
time (ps)